



This is a repository copy of *Morphology of a human finger pad during sliding against a grooved plate: A pilot study.*

White Rose Research Online URL for this paper:
<https://eprints.whiterose.ac.uk/154825/>

Version: Accepted Version

Article:

Lee, Z.S., Maiti, R., Carre, M. et al. (1 more author) (2020) Morphology of a human finger pad during sliding against a grooved plate: A pilot study. *Biotribology*, 21. 100114. ISSN 2352-5738

<https://doi.org/10.1016/j.biotri.2019.100114>

Article available under the terms of the CC-BY-NC-ND licence
(<https://creativecommons.org/licenses/by-nc-nd/4.0/>).

Reuse

This article is distributed under the terms of the Creative Commons Attribution-NonCommercial-NoDerivs (CC BY-NC-ND) licence. This licence only allows you to download this work and share it with others as long as you credit the authors, but you can't change the article in any way or use it commercially. More information and the full terms of the licence here: <https://creativecommons.org/licenses/>

Takedown

If you consider content in White Rose Research Online to be in breach of UK law, please notify us by emailing eprints@whiterose.ac.uk including the URL of the record and the reason for the withdrawal request.



eprints@whiterose.ac.uk
<https://eprints.whiterose.ac.uk/>

1 **Morphology of a human finger pad during sliding against a grooved plate (pilot study?)**

2 Zing Siang Lee^{1*}, Raman Maiti¹, Matt Carre¹, Roger Lewis¹

3 ¹*Department of Mechanical Engineering, University of Sheffield, Sheffield, UK*

4 *corresponding author: z.s.lee@sheffield.ac.uk

5 Keywords: finger pad; grooved plate; sliding interaction; optical coherence tomography

6 **Abstract**

7 This pilot study shows that Optical Coherence Tomography can be used to capture the
8 morphology of the finger pad during sliding interaction with a grooved plate. The videos show
9 how the finger pad ridges deform to slide or compress closer to the edge of the grooves. This
10 study has demonstrated the future possibilities of investigating and visualising the interaction
11 of a finger pad with a plate specimen of controlled roughness to improve and optimise surface
12 characteristics of consumer products.

13 **1 Introduction**

14 In recent years, considerable work has been done to study the interaction between human
15 skin and counter-face materials with different roughness. Tomlinson et al. [1][2] measured
16 the forces produced when a finger pad interacts with triangular and rectangular ridged
17 counter-face materials respectively. In the study of finger pad interaction with a triangular
18 ridged counter-face material, Tomlinson et al. [1] have shown that adhesion was the
19 predominant friction mechanism for shallow triangular ridges while interlocking with finger
20 pad ridges was more influential for higher triangular ridges. Also, Tomlinson et al. [2] found
21 that the sliding of a finger pad across a rectangular ridged counter-face could be classified
22 into 4 stages of friction evolution. The main friction mechanisms were adhesion, ploughing
23 friction and/or the reformation (hysteresis) of the finger pad depending on which sliding stage.

24 Derler et al. [3] found that the frictional behaviour of human skin (hand and finger) varied in
25 response to the glass specimens with different surface roughness and contact conditions
26 (dry/wet). In addition, Derler and Gerhardt [4] also reviewed various parameters influencing
27 the friction coefficient of human skin, which includes the surface roughness of contacting
28 materials. Other studies such as Delhaye et al. [5] studied the surface strain of finger pad in
29 sliding contact and Liu et al. [6] studied the apparent and real contact of finger pad using
30 Optical Coherence Tomography.

31 These studies have established the potential friction mechanisms during the finger pad and
32 ridged material interaction using experimental and modelling. However, there is still a lack of
33 clarity in the extent of which individual friction mechanisms are at play because there is little
34 visualisation of the interaction. Visualisation is helpful in identifying the friction mechanisms

35 between finger pad and a transparent counter-face material. Visualisation is especially
36 suitable for the friction mechanisms that involve with the deformation of human skin because
37 these mechanisms are dictated by the surface roughness and the surface geometry of the
38 counter-face material. In addition, adhesion friction mechanism is visualised easily during the
39 state transition of human skin from static to dynamic. For example, the contacting surface of
40 human skin remains in contact with a smooth counter-face material without breaking off and
41 sliding while the sub-surface of human skin has moved. Therefore, a method for visualising
42 the edge interaction between a finger pad and a counter-face material is needed.

43 Optical Coherence Tomography (OCT) has recently been used to study finger-pad skin surface
44 and sub-surface strain during sliding [7], sub-clinical assessment using angiography to assess
45 severity of skin suffering with atopic dermatitis [8], changes on eye/eye-lid surface during
46 contact lens interaction [9] and morphological parameters changes of forearm skin during
47 natural stretching [10]. As such, the aim of this study was to investigate the feasibility of using
48 an OCT system to capture the morphological changes of finger pad ridges across a counter-
49 face material with an uneven surface. The required quality of the captured images was
50 deemed to be the level that would show how the skin deforms around the grooves from the
51 static state to the dynamic state.

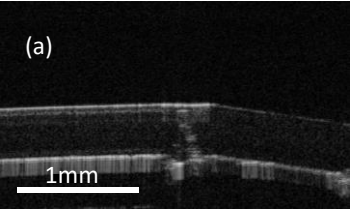
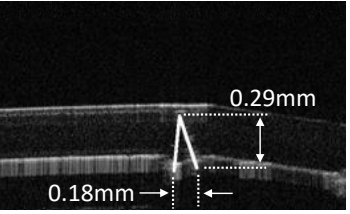
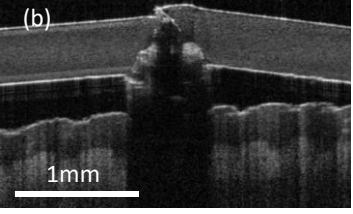
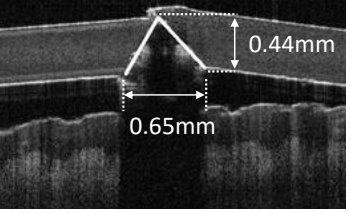
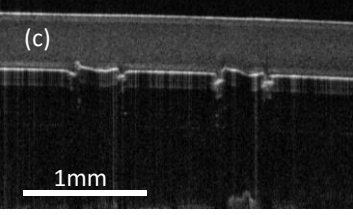
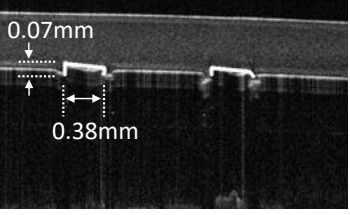
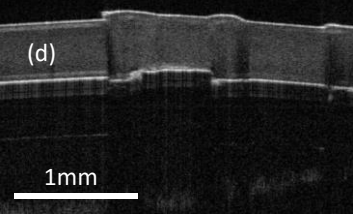
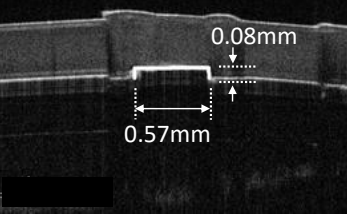
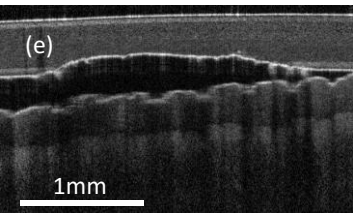
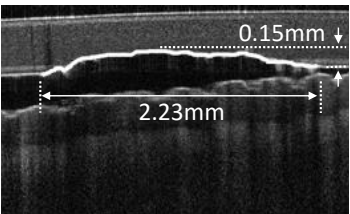
52 **2 Materials and Methods**

53 ***2.1 Test subject and plate specimens***

54 The test subject was a male, aged 26 years old. The experiment was done on the subject's left
55 index finger in a natural state without any pre-treatment. The environmental conditions
56 during the test were around 20°C and 45-50 % relative humidity. The protocol of the study
57 was approved by The University of Sheffield (Ethics Number 002074).

58 Transparent contact plate specimens were manufactured from polypropylene with an
59 average thickness of 455µm. Grooves were made by sliding a knife across the plastic plate.
60 The specimens are summarised in Figure 1. Videos showing the sliding interaction between
61 the finger pad and various grooved plates are made available on Biotribology Journal (Elsevier)
62 labelled as: Figure 1(a) - Small triangular groove, Figure 1(b) - Big triangular groove, Figure 1(c)

63 - Small rectangular grooves, Figure 1(d) - Big rectangular groove, Figure 1(e) - Big curved
 64 groove.

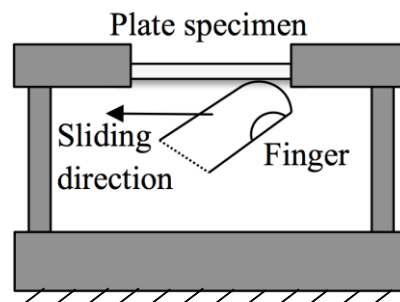
Groove Type	Respective OCT image	
Small "triangular" groove		
Big "triangular" groove		
Small "rectangular" grooves		
Big "rectangular" groove		
Big "curved" groove		

65

66 Figure 1: Images obtained for a finger in contact with different types of grooves using OCT
 67 and the dimensions of the grooves

68 **2.2 Experimental protocols**

69 The plate specimen (counter-face) was held using a support rig, as shown in Figure 2, while
70 the finger pad was slid against it. The normal force and sliding speed were kept constant at
71 around 2N and 2mm/s respectively throughout the experiment.



72

73 Figure 2: Experimental set-up of finger pad sliding against plastic specimen

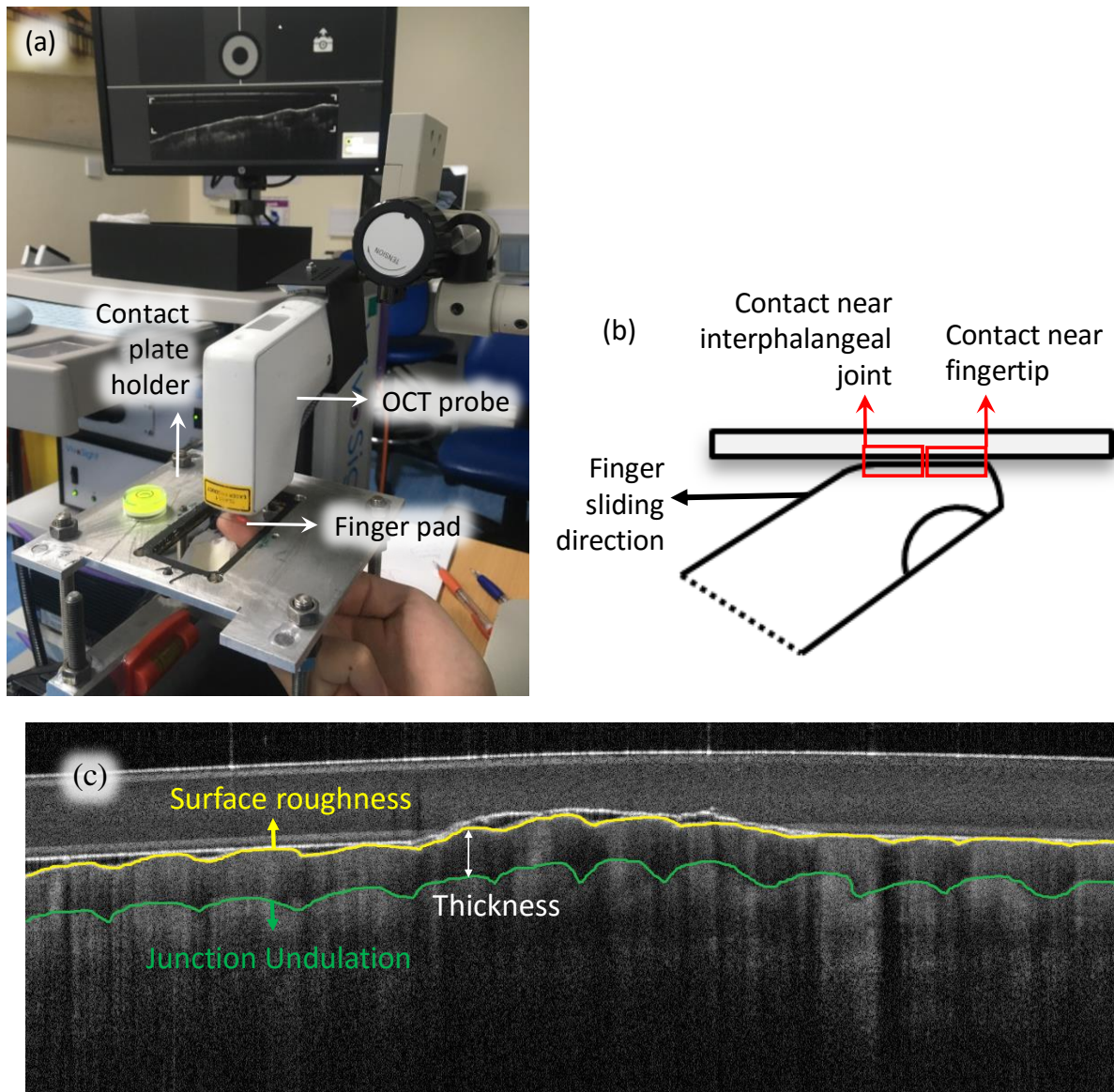
74 **2.3 Optical Coherence Tomography**

75 Optical Coherence Tomography (OCT) is a non-invasive imaging technique that can capture
76 images showing surface and subsurface morphology of biological tissues. A clinically-
77 approved Vivosight® OCT system (Michelson Diagnostics, Kent) has a Fourier domain with a
78 20 kHz swept source laser at 1300 nm centre wavelength, 7.5 μm lateral and 5 μm axial
79 resolution. This system was used to visualise the interaction between the finger pad and a
80 plate specimen from the static state to the dynamic state. Continuous B-scans [11] were
81 captured to identify the cross-sectional image of the specimen in real-time. The image
82 capturing rate was 20 frames per second and the resolution of each image was 1342 \times 460
83 pixels. The OCT assembly (shown in (a)) was similar to that used in the study by Maiti et al.
84 [10] in assessing deformation in forearm skin during natural stretching.

85 Videos for each grooved specimen were captured before and during finger pad contact with
86 the plates and at two positions of the finger pad, close to the finger-tip and over the
87 interphalangeal joint. Each video was converted into a total of 194 Images using the “image
88 sequence function” in ImageJ [12].

89 Morphological parameters (thickness of stratum corneum, top surface roughness and
90 stratum corneum – stratum lucidum undulation as shown in Figure 3(c)) were computed from
91 six consecutive OCT images at each of the following conditions: no contact, contact near
92 interphalangeal joint and contact near fingertip as shown in Figure 3 (b). This is done using an

93 image processing algorithm presented by Maiti et al. in [10]. The parameters are presented
94 as mean \pm standard deviation for each condition.



95

96

97 Figure 3: (a) OCT system assembly, (b) location of OCT images where the morphological
98 images were computed and (c) illustration of morphological parameters

99 3 Results

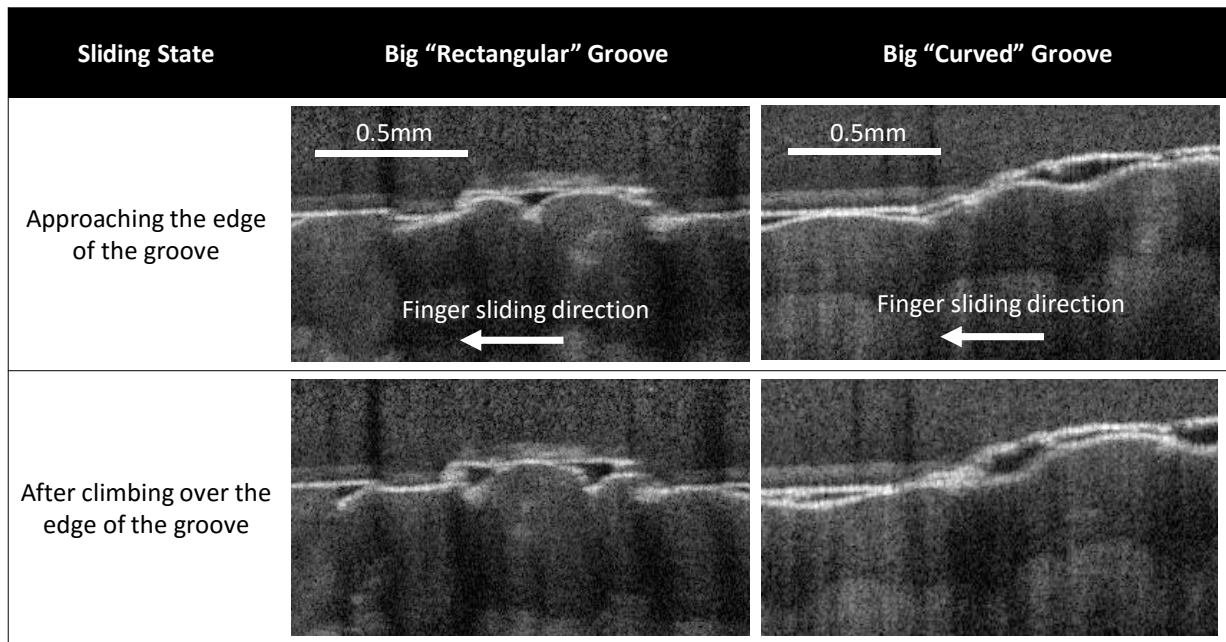
100 3.1 Morphological change of finger pad against grooved plate during sliding

101 Videos, available on Biotribology Journal (Elsevier), show the morphological changes of the
102 finger pad when it was slid against the grooves. Figure 4 shows how the finger ridge deformed
103 when approaching and climbing over two groove specimens that have different edge

104 geometry. The edge of the big “rectangular” groove has a rectangular and pointy edge while
105 the edge of big “curved” groove is curved and has a rounded edge. In the first case, the finger
106 ridge deformed and ploughed by the edge of the groove when approaching the edge. Then,
107 the finger ridge returned to its flattened contact after climbing over the edge of the groove.
108 In the latter, the finger ridge did not seem to deform much in terms of interlocking or
109 ploughing.

110 The thickness of stratum corneum near to the interphalangeal joint reduced by 20% from
111 322.8 μm to 257.6 μm during sliding through the big “curved” groove as shown in Figure 5.
112 This thickness increases significantly by 50% when the region of interest of the finger pad skin
113 interaction with groove changes from skin closer to interphalangeal joint to skin closer to
114 fingertip. Similarly, the surface roughness and stratum corneum – stratum lucidum junction
115 undulation also significantly decreases from 5.17 μm to 2.36 μm and significantly increases
116 from 4.41 μm to 6.70 μm by a factor of 50%. There was no significant difference in surface
117 roughness or junction undulation between skin near fingertip and interphalangeal joint.

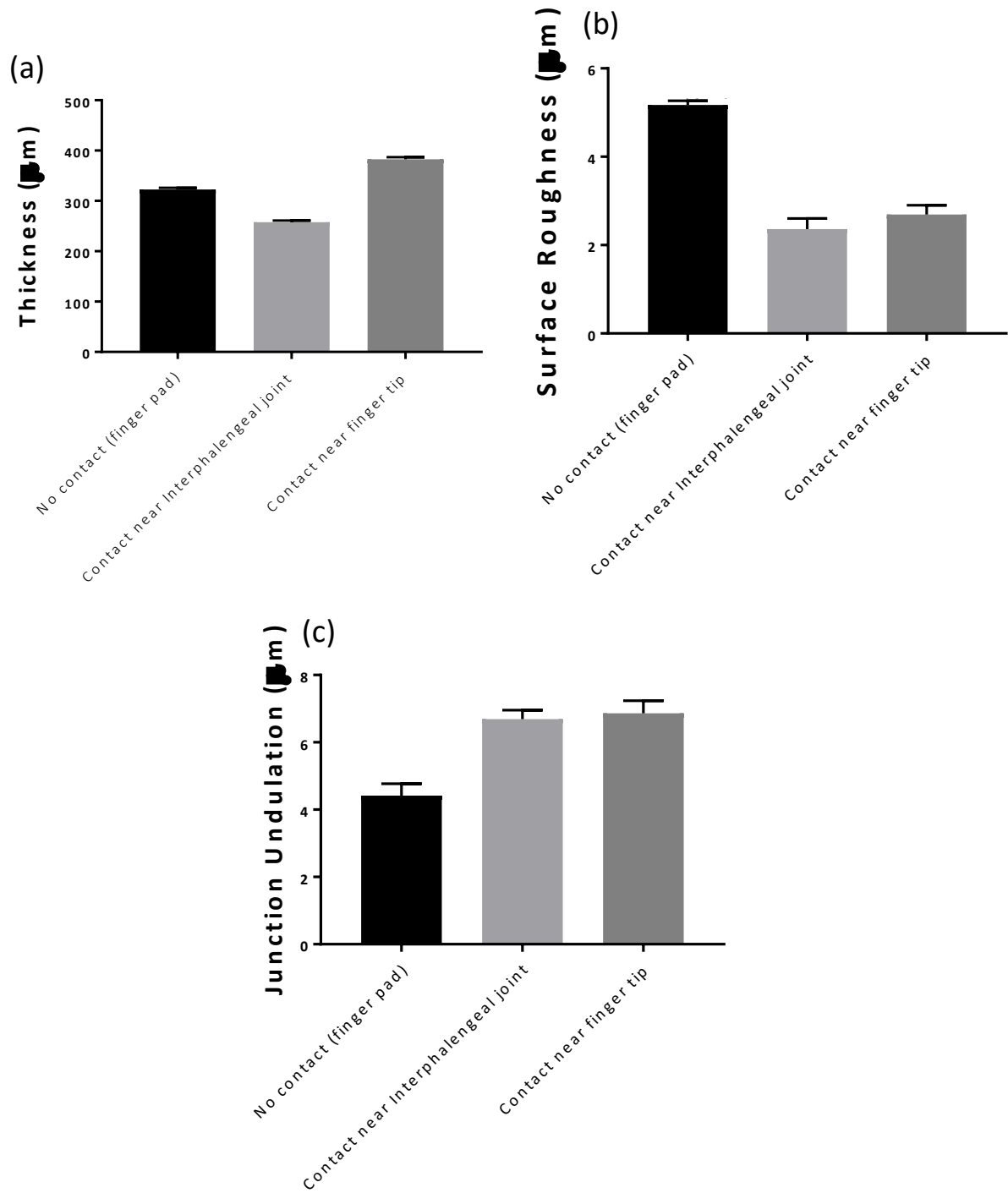
118 Smaller grooves such as small “triangular” and “rectangular” grooves did not show any
119 significant effect on the finger pad skin deformation (videos available electronically Figure 1(a)
120 and (c)). As the width of the groove increased, the finger pad skin was affected by the grooves.
121 There was distinctive loss of visualisation in OCT images of big “triangular” groove, highlighted
122 in red circle shown in Figure 6. The extent of the image loss varies with the different grooves.
123 The big “triangular” groove OCT images suffered the most loss of visualisation because the
124 lights were not reflected properly due to sharp bend not giving a clear image of the finger pad
125 skin.



126

127
128

Figure 4: Images of the deformation of finger ridges on interaction with the edge of a "rectangular" and a "curved" groove plate specimen.

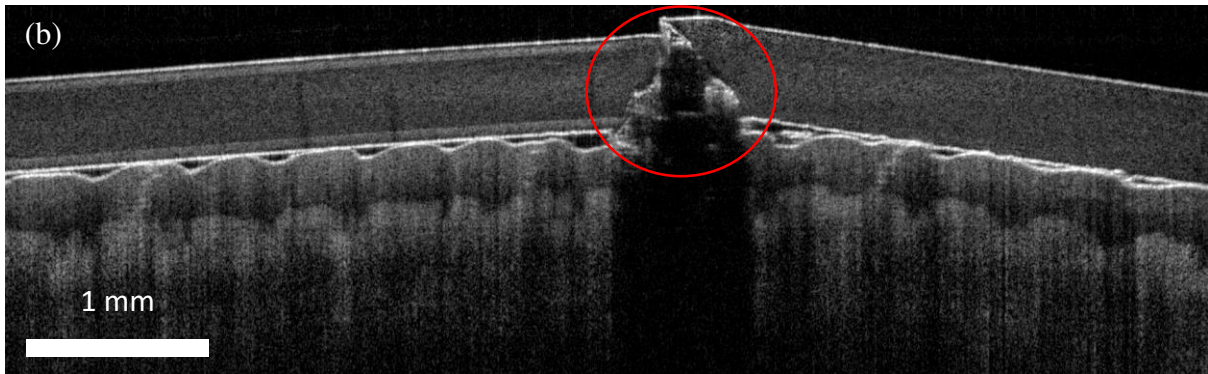
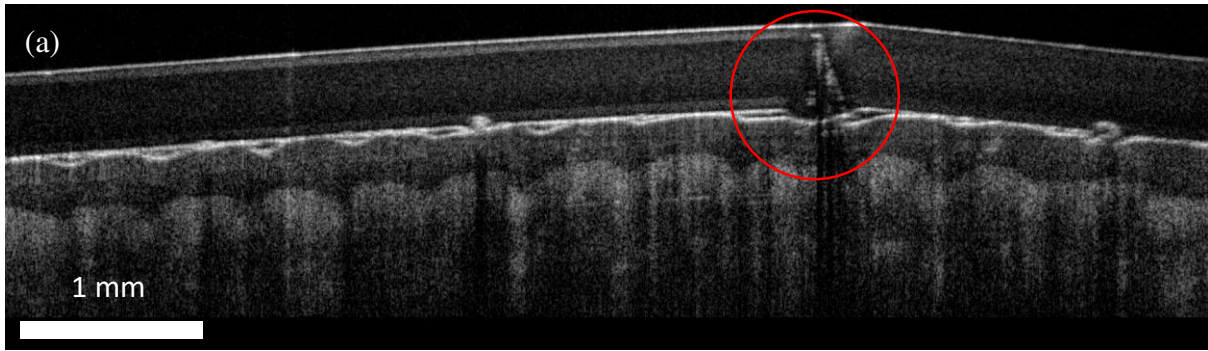


129

130

131

Figure 4: (a) thickness, (b) surface roughness and (c) stratum corneum – stratum lucidum junction undulation of finger pad skin at no contact and during sliding with big curve groove.



134 Figure 5: OCT image with (a) partial image loss and (b) total image loss

135 **4 Discussion**

136 The thickness of the finger pad near interphalangeal joint reduced on the application of
137 normal load. However, the increase in thickness closer to finger pad can be attributed to the
138 bulging of the skin layer near the tip. The decrease in the gap between finger ridges and plate
139 resulted in higher roughness in both positions of the finger pad. The increase in junction
140 undulation within the sub-surface of finger pad may due to the friction during sliding.

141 **4.1 Friction mechanisms**

142 When the finger pad was sliding against the plate specimen with big “curved” groove, the
143 interlocking effect or ploughing friction effect on the finger pad were not obvious because the
144 edge of the groove was more rounded and circular. Therefore, adhesion seems to be the
145 predominant friction mechanism of the finger pad sliding interaction, which is similar to the
146 sliding interaction between a finger pad and a shallow triangular ridge in a study by Tomlinson
147 et al. [1]. On the other hand, the finger pad ridges were ploughed by the edge of the groove
148 when sliding against the plate specimen with the big “rectangular” groove. The was due to
149 the rectangular shape edge that provides a platform to plough .

150 The importance of the geometry of the edge of the groove is shown because the friction
151 mechanisms of a finger pad are different between a “rectangular” and a “curved” groove
152 plate. This could extend to the dimensions of the triangular, rectangular and curved grooves
153 because the width and the depth of the grooves will affect the frictional behaviour of finger
154 pad and the predominant friction mechanisms. This study attempted to investigate the role
155 of groove dimensions as shown in the small and big “rectangular” groove plate specimens.
156 Both have the same ploughing phenomenon at the edge of the groove although it is less
157 obvious in the small “rectangular” groove video due to the partial image loss under the edge
158 of the groove.

159 **4.2 Feasibility of OCT in studying finger pad – grooved plate interaction**

160 Although this pilot study mostly studies the visual results of the experiments, it has
161 successfully shown that OCT system can be used to study the morphological change of the
162 finger pad ridges when sliding across the grooves of the plate specimens.

163 Most videos show partial or total image loss regions under the grooves. These regions were
164 caused by the light diffraction phenomenon as OCT relies on the light reflection signal to
165 produce the OCT images. It is also observed that these regions normally occurred at the
166 grooves that have a sudden change of plate thickness. In the case of the big “curved” groove-
167 finger pad sliding interaction, there are no image loss regions because the plate thickness did
168 not decrease as dramatically as other grooves that gave severe light diffraction.

169 **5 Conclusions and Future work**

170 This experiment has shown the feasibility of using an OCT system to visualise the finger pad
171 sliding interactions with plate specimens of different grooves. It has shown the possibilities
172 to investigate the interaction of finger pad with plate specimen of controlled surface
173 roughness.

174 Due to the methodology in manufacturing the grooves was very crude, the future work will
175 need to focus on developing a manufacturing method that can make plate specimens with
176 grooves in a controllable manner. This would help in determining the baseline of the depth
177 and the width of the grooves when the image loss becomes significant. Only when the image
178 quality of the OCT images is acceptable and consistent, the roughness of the groove and the

179 finger pad can be accurately measured and post-processed. Then, this could be tested in a
180 large pool of participants in the future when the testing methodology is stable. With the
181 information on the friction mechanism and skin deformation, it can help us in designing better
182 consumer product and understand the gripping method and sports biomechanics interactions.

- [1] Tomlinson, SE, Carré, MJ, Lewis, R, Franklin, SE. Human finger contact with small, triangular ridged surfaces. *Wear*. 2011; **271**: 2346-2353.
- [2] Tomlinson, SE, Carré, MJ, Lewis, R, Franklin, SE. Human finger friction in contacts with ridges surfaces. *Wear*. 2013; **301**: 330-337.
- [3] Derler, S, Gerhardt, L-C, Lenz, A, Bertaux, E, Hadad, M. Friction of human skin against smooth and rough glass as a function of the contact pressure. *Tribology International*. 2009; **42**: 1565-1574.
- [4] Derler, S, and Gerhardt, L-C. Tribology of skin: review and analysis of experimental results for the friction coefficient of human skin. *Tribology Letter*. 2012; **45**: 1-27.
- [5] Delhaye, B, Barrea, A, Edin, BB, Lefevre, P, Thonnard, J-L. Surface strain measurements of fingertip skin under shearing. *Journal of Royal Society of Interface*. **13**; 20150874.
- [6] Liu, X, Maiti, R, Lu, ZH, Carré, MJ, Matcher, SJ, Lewis, R. Measuring contact area in a sliding human finger-pad contact. *Skin Research Technology*. 2017; 1-14.
- [7] Liu, X, Maiti, R, Lu, ZH, Carré, MJ, Matcher, SJ, Lewis, R. New non-invasive techniques to quantify skin surface strain and sub-surface layer deformation of finger-pad during sliding. *Biotribology*. 2017; **12**: 52-58.
- [8] Byers, RA, Maiti, R, Danby, SG, Pang, EJ, Mitchel, B, Carré, MJ, Lewis, R, Cork, MJ, Matcher, SJ. Sub-clinical assessment of atopic dermatitis severity using angiographic optical coherence tomography. *Biomedical Optics Express*. 2018; **9**: 2001-2017.
- [9] Morecroft, R, Toomey, P, Goff, JE, Mylon, P, Carré, MJ, Matcher, SJ, Lewis, R, Maiti, R. Investigation into surface interaction between the contact lens and the upper eyelid margin using optical coherence tomography. *SPIE Conference*. Feb 2017, California, USA.
- [10] Maiti, R, Gerhardt, L-C, Lee, ZS, Byers, RA, Woods, D, Sanz-Harrera, JA, Franklin, SE, Lewis, R, Matcher, SJ, Carré, MJ. In vivo measurement of skin surface strain and sub surface layer deformation induced by natural tissue stretching. *Journal of the Mechanical Behaviour of Biomedical Materials*. 2016; **62**: 556-569.
- [11] Kraus, MF, Potsaid, B, Mayer, MA, Bock, R, Baumann, B, Liu, JJ, Hornegger, J, Fujimoto, JG. Motion correction in optical coherence tomography volumes on a per A-scan basis using orthogonal scan patterns. *Biomedical Optics Express*. 2012; **3**: 1182-1199.
- [12] Rueden, CT, Schindelin, J, Hiner, MC, et al., [ImageJ2: ImageJ for the next generation of scientific image data](#). *BMC Bioinformatics* 2017; **18**: 529. [PMID 29187165](#), doi:[10.1186/s12859-017-1934-z](#)

